EFFECT OF NOZZLE CONFIGURATION ON PERFORMANCE OF A SPRAY DRYER

Ashraf Ali Basheer[1], Singh Sunil Kumar[2]

Complex Fluid Flow and Visualization Research Lab
Department of Chemical Engineering
National Institute of Technology Karnataka
Mangalore, India 575025
E-mail: ashrafali@nitk.edu.in

Received 18 October 2022
Accepted 12 May 2023
DOI: 10.59957/jctm.v59.i1.2024.14

ABSTRACT

In this work, hydrodynamics and drying characteristics of spray dryer is numerically investigated using computational fluid dynamics (CFD) using Euler-Lagrangian (EL) approach. The gas phase is modelled as the continuous phase and solid particle as the dispersed phase. The turbulence in the gas phase is predicted using RNG version of k-ε model. As air flow pattern influences the time spent by particle in drying chamber, the spatial variation of air velocity and its circulation rate is quantified. Accordingly, optimum conditions for drying the feed slurry are determined. Further, five different outlet pipe locations are chosen and the optimum location is identified which supports the highest evaporation rate. To improve the product quality, conventional nozzle is modified and particle impact positions are analyzed. The particles impact positions on the dryer's surface are found to be minimum for the proposed nozzle configuration and it improves the final product quality.

Keywords: Euler-Lagrangian approach, CFD, hydrodynamics, evaporation, spray dryer.

INTRODUCTION

Spray drying is an important energy-intensive unit operation in chemical, pharmaceutical and food industries. In spray-drying, an atomized spray is contacted with a drying medium either in a co-current or counter-current mode and evaporation takes place. This gives dried particles which are subsequently separated from the drying medium (gas stream). Spray dryers are used for the production of maltodextrin concentrate in powdered form from its aqueous solution. The maltodextrin concentrate is commonly used in food industries to enhance their flavor, shelf life and texture. This also provides thickness to the food and replaces sugar in foods. The production of maltodextrin from its slurry and its concentration in a spray dryer is still a challenge due to its highly cohesive property.

Although a large number of studies are reported on the spray drying operation in the literature, very little work was focused on understanding the impact of operating conditions on denaturation and solubility of maltodextrin. Since the measurements of temperature distribution, airflow velocity, particle size distribution and humidity are very difficult in the spray drying operation. These parameters are used to characterize the performance of spray drier in the present work.

The CFD models such as Euler-Eulerian (EE) and Euler-Lagrangian (EL) are used to obtain flow pattern in a spray drier. In EE approach, the continuous (gas) and dispersed (particles) phases are treated as interacting and interpenetrating continua [1]. In EL approach, the hot air (gas phase) is modeled as a continuum and the feed slurry (maltodextrin) is treated as discrete particles. These solid particles are tracked in the Lagrangian framework [2, 3]. As the Euler- Lagrangian approach accurately predicts the gas temperature, its velocity profile and droplet evaporation [2, 4 - 6], in the present work, the hot air (gas) and the feed slurry (maltodextrin) are modelled

as continuous and dispersed phase, respectively. The injected solid particles are treated in the Lagrangian frame of reference using Newton's 2nd law of motion [2].

In a spray-drying operation, there are millions/ billions of particles in the spray chamber. The trajectories of all such particles are modelled using the dispersed phase model (DPM) through commercial CFD software (ANSYS Fluent v2020 R2). The dispersed phase model treats each particle as a parcel of particles. These particles are subjected to forces such as drag, pressure in addition to gravity.

Saleh & Amjad performed CFD simulations using the Lagrangian approach [7]. They found that the quality and final dried product morphology depend on the hydrodynamics in the spray dryer. Cher Pin et al. investigated gas-solid flow in a spray dryer using different turbulence models (standard, realizable k-ε and RNG) and found that RNG k- ε turbulent model accurately predicts swirl flows [5]. Saleh & Amjad used 3D CFD simulations to predict heat and mass transfer characteristics in a co-current flow spray dryer using RNG version of k-ε model [8]. They quantified the flow pattern using a digital anemometer. Patil et al. found that air temperature at the inlet significantly influences the extent of moisture in the product [9].

Ali et al. investigated the air flow pattern, particle moisture content, and particle size in a spray dryer [10]. They found that the air flow pattern affects the particle impact positions on the dryer surface. Saha et al. studied the effect of air temperature (inlet), feed injection rate on the outlet temperature (product) and efficiency of the dryer[11]. They found that the efficiency of the dryer decreases when air temperature at the inlet increases.

The particle impact position and particle stickiness are the most conventional problems that limit the spray drying of food products. This significantly influences the flow ability and bulk density of dried solid particles. Thus, the knowledge of accurate prediction of particles histories on dryer's surface is necessary to improve the quality of dried product. This needs to be analyzed for a wide range of operating parameters as it influences the stickiness conditions of dairy products. In this regard, the glass transition temperature is used as an indicator for stickiness. Adhikari et al. used glass transition approach to find the particle stickiness on the surface of the wall [12]. They found that the stickiness of the particles on the spray dryer's surface depends on the extent of moisture content of the solid particles and their temperature. Further, Gianfrancesco et al. identified the sticky zones inside the spray dryer using the glass transition temperature approach [13].

To improve the product quality during the spray-drying operation, Saleh & Amjad [8] used an atomizer in the spray dryer and analyzed the drying kinetics. They found that the atomizer creates swirling flows. Francia et al. used counter-current spray drier (with nozzle) to study the agglomeration kinetics of particles [14]. They found that the position of the nozzle supports a wide range of product size and promotes the elutriation of powder.

In most of the published papers, EL approach is used to predict the air temperature and its velocity profile. The problems in spray drying operations are associated with the prediction of particle temperature, shape and size. These influence the bulk density of the dried product and its flow ability a spray dryer. In most of the models, variations in temperature of the air, the residence time, the flow of solid particles are neglected. Thus, the performance of spray dryer has not been predicted accurately. Hence, in the present work, these effects are considered in the CFD model, accordingly the performance of the spray dryer is characterized. The effects of gas temperature, gas velocity, air outlet pipe location, particle size on air flow pattern and drying characteristics of feed slurry (maltodextrin) have been investigated to determine the optimum operating conditions in the spray dryer. The nozzle configuration is modified to enhance the performance of spray drier.

The article is organized by discussing geometry of the spray dryer at first. Followed by the computational modelling and simulation methodology were discussed. Subsequently, the predicted flow pattern and the influence of various operating, geometric parameters on the performance of spray dryer are discussed. Finally, the key findings are summarized.

EXPERIMENTAL

Geometry of the spray dryer

The geometry of the co-current spray dryer is shown in Fig. 1. It consists of a cylindrical vessel with 224 mm diameter and 205 mm height. The height of the cone is 175 mm. The hot air is introduced through the annulus, co-current to the feed inlet. The hydraulic diameter of the

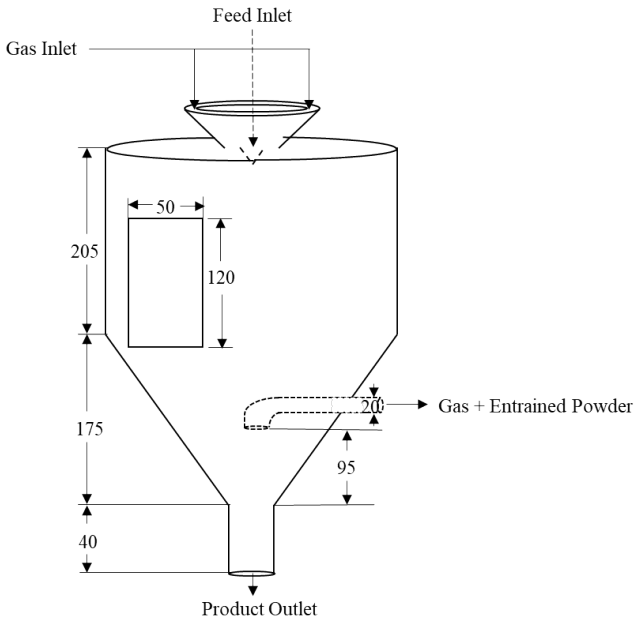

Fig. 1. Schematic of the spray dryer (mm).

air inlet is 43 mm. The feed slurry is injected through a nozzle of diameter 0.2 mm and at an angle of 45° from the top of the column.

Computational Modeling

The hydrodynamics and drying characteristics of feed slurry (maltodextrin) in a dryer are numerically investigated through Euler-Lagrangian approach [16]. Here gas phase is modelled as the continuous phase and feed slurry (maltodextrin) is treated as discrete particles. The flow field (gas) is calculated using Eulerian approach and it is governed by the time averaged continuity, momentum equations.

$$\frac{\partial \rho}{\partial t} + \nabla.(\rho \vec{u}) = 0 \tag{1}$$

$$\frac{\partial(\rho u_i)}{\partial t} + \frac{\partial}{\partial x_j}(\rho u_i u_j) = -\frac{\partial p}{\partial x_i} + \\ + \frac{\partial}{\partial x_j}\left[\mu\left(\frac{\partial u_i}{\partial x_j} + \frac{\partial u_j}{\partial x_i} + \frac{2}{3}\delta_{ij}\frac{\partial u_k}{\partial x_k}\right)\right] + \frac{\partial}{\partial x_j}\left(-\rho\overline{u_i' u_j'}\right) \tag{2}$$

where, ρ is the density, μ is the viscosity, δ_{ij} is the Kronecker delta function, $\overline{u_i' u_j'}$ is the Reynolds stress (additional unknown) and p is the pressure term.

In a spray dryer, the swirl flow influences heat and mass transfer characteristics between the phases. This is modelled using RNG version of the k-ε model [5,17]

$$\frac{\partial}{\partial t}(\rho k) + \frac{\partial}{\partial x_i}(\rho k u_j) = \frac{\partial}{\partial x_j}\left[\left(\mu + \frac{\mu_t}{\sigma_k}\right)\frac{\partial k}{\partial x_j}\right] - G_k - \rho\varepsilon \tag{3}$$

$$\frac{\partial}{\partial t}(\rho\varepsilon) + \frac{\partial}{\partial x_j}(\rho\varepsilon u_j) = \frac{\partial}{\partial x_j}\left[\left(\mu + \frac{\mu_t}{\sigma_\varepsilon}\right)\frac{\partial \varepsilon}{\partial x_j}\right] + \\ + C_{1\varepsilon}\frac{\varepsilon}{k}G_k - C_{2\varepsilon}^{*}\rho\frac{\varepsilon^2}{k} \tag{4}$$

The RNG k-ε model constant values are [17]:

$C_\mu = 0.0845$; $C_{\epsilon 1} = 1.42$; $C_{\epsilon 2} = 1.68$;
$\sigma_k = 1.39$; $\sigma_\epsilon = 1.68$.

Based on gas phase solution, trajectories of dispersed phase (particles) are obtained by solving Newton's 2nd law of motion for individual particles:

$$\frac{d\vec{u}_p}{dt} = F_d(\vec{u}_p - \vec{u}_p) + g\left(\frac{\rho_p - \rho}{\rho_p}\right) \tag{5}$$

The 1st term on the RHS of (5) represents drag force, 2nd term accounts for buoyancy force. The drag force is obtained by:

$$F_d = \frac{18\,\mu}{\rho_p d_p^2}\frac{C_D\,Re}{24} \tag{6}$$

where Re is the particle Reynolds number, ρ_p is the density of particle (kg m^{-3}); *dp* is the diameter of particle (μm) and C_D is the drag coefficient.

The vaporization rate that accounts vapor at the droplet surface and vapor in the gas phase is computed using:

$$N_i = k_c(C_{i,s} - C_{i,\infty}) \tag{7}$$

The following Sherwood number correlation is used to calculate mass transfer coefficient in (7):

$$Sh = \frac{k_c d_p}{D_i} = 2.0 + 0.6Re^{1/2}Sc^{1/2} \tag{8}$$

where Re stands for particle Reynolds number, *Sc* denotes for Schmidt number, D_i is diffusion coefficient (vapor in the bulk) and d_p is the particle diameter.

Here, vaporization of the volatile substance takes place when droplet temperature reaches the vaporization temperature (T_{vap}). In this drying period, heat transfer takes place from dry air to the surface of the droplet due to convection. This leads to evaporation of the free moisture from the feed slurry. The transport equations and other details are obtained from the literature [16].

Simulation Methodology

The hydrodynamics and drying characteristics of feed slurry (maltodextrin) in a spray dryer (co-current) are predicted using commercial CFD software (ANSYS 2019 R2). Here, the geometry of the spray dryer is modelled using ANSYS workbench for three grid sizes (tetrahedral mesh), such as 1,00,000, 3,00,000, and 5,00,000. The CFD predictions are checked for grid independence (optimum: 3,00,000). The mass flow rate boundary condition (BC) is imposed at the inlet. At the outlet of the spray drier pressure outlet BC is specified. The atomizer is modelled by specifying the mass flow rate, components of velocity and particle size. The no-slip BC is applied at the walls of the spray dryer. The overall heat transfer coefficient at the wall is determined from the energy balance over the dryer. The trap BC is imposed to the particles that hit the dryer's walls and the reflect BC is specified to the particles at the feed inlet. The convective terms are discretized using 2nd order upwind scheme. The SIMPLE algorithm is used to couple pressure-velocity. The CFD simulations are performed using the discrete phase model (DPM) with time step, Δt = 0.01s (optimum).

RESULTS AND DISCUSSION

The flow field in a spray dryer is predicted using transient 3D CFD simulations. The vertical plane (z = 0 m) is chosen and contours of gas velocity is analysed at various time instants (Fig. 2). Here, velocity magnitude (air) is found to be zero at t = 0s and its magnitude is increases when t > 0s. The air velocity is found to be high at the centre and minimum near the periphery of dryer walls. A recirculation zone is observed at the bottom of the dryer and it leads to an increase in particle residence time.

The horizontal lines are chosen along the height of the spray dryer to quantify the flow field. The spatial variation of normalized air velocity is analyzed along these lines. This is shown in Fig. 3. The normalized velocity is found to be high at the core region of the spray chamber. The predicted gas flow pattern is observed to be symmetric at the upstream level (y = 0.03 m) and asymmetric in the downstream level (y = 0.06 m) of dryer. These predictions are validated with experimental data of Saleh and found to be consistent [7]. The calculated error between experimental and numerical predictions is found to be approximately 12 %.

To find an optimum temperature in the spray dryer, the irreversibility induced by the air flow is quantified using the air circulation rate. This is calculated by taking the line integral of the velocity field over the flow domain [18]:

$$\Gamma = \oint v.dl \tag{9}$$

where Γ is the air circulation rate, *dl* is a small differential element, v is the velocity vector.

The flow domain chosen for the calculation of air

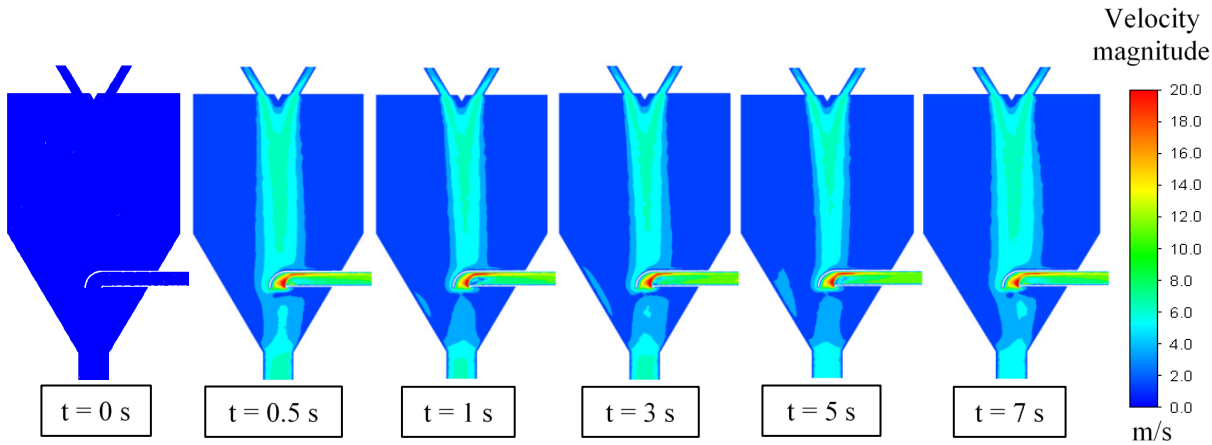

Fig. 2. Iso-contours of air velocity magnitude at different time instants (inlet air temperature = 350 K; velocity = 7 m/s).

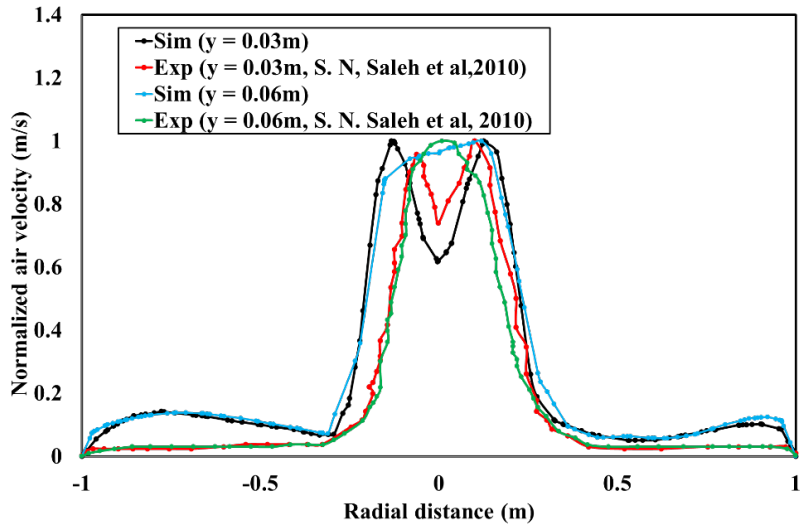

Fig. 3. Spatial variation of air velocity with radial distance.

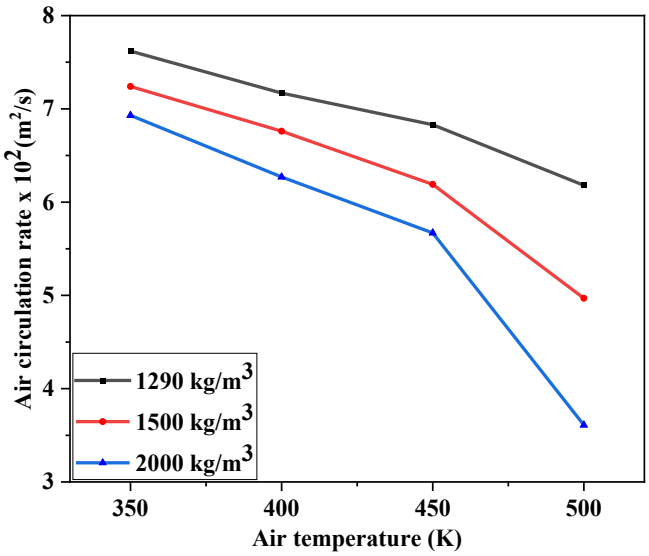

Fig. 4. Effect of air temperature on air circulation rate.

circulation rate is shown in Fig. 1. The air circulation rate is analysed for various densities of feed slurries and hot air temperatures (Fig. 4). It is observed that circulation rate (air) decreases when air temperature increases. This is attributed to the resistance offered by feed slurry (maltodextrin) on the gas flow pattern. The calculated air-circulation rate is found to be high when 350 K is used. Hence, this temperature is considered optimum for the operation of the co-current spray dryer.

This is further verified by analysing predicted particle residence time (feed slurry) and it is obtained by tracking particle trajectories in the flow domain. The particles residence time for various hot air temperatures is shown in Table 1.

It is observed that the particle residence time is decreases as the hot air temperature increases due to water evaporation from feed slurry into hot air. The particle residence time is found higher at 350 K (hot air temperature). This observation once again confirms the predicted optimum air temperature (350 K). As the

flow pattern in the spray dryer depends strongly on the product outlet pipe location, five different air outlet pipe locations are considered at the bottom of the spray dryer, Fig. 5(a) - 5(e). Its effect on the air circulation rate and the evaporation rate are calculated. This is reported in Table 2.

The air circulation rate is observed to be higher when air outlet pipe location (a) is used as it does not reduce the available area for gas recirculation. However, the predicted evaporation rate is found to be the same for all air outlet pipe locations. This is because the inlet air temperature is maintained the same. Since air circulation rate is found to be higher when air outlet location (a) is used, the spray dryer with air outlet location (a) is considered to be optimum air outlet pipe location.

Table 1. Effect of air temperature on the residence time of particle.

Air temperature, K	Particle residence time (10^2, s)
350	3.79
400	3.76
450	3.55
500	3.44

Table 2. Effect of air outlet location on the air circulation rate and evaporation rate.

Air Outlet	Air circulation rate (10^2, $m^2\ s^{-1}$)	Evaporation rate (10^4, kg s^{-1})
a	12.23	1.1
b	10.03	1.1
c	7.62	1.1
d	-3.00	1.1
e	-3.70	1.1

The performance of the optimized spray dryer is further analysed by considering various initial moisture contents of the feed slurry (density = 1290 kg m^{-3}; particle size = 100 μm) at the optimized conditions (350 K). Its effect on the evaporation rate, particle residence time and particle deposition on the various sections of the dryer are calculated and reported in Table 3. As observed, the evaporation rate of the final product increases with an increase in the initial feed moisture content as it has higher volatile substances. The magnitude of evaporation rate is found to be higher when initial feed moisture of 9 kg_w/kg_f is used. This is attributed to the volatility of the feed slurry. Further, particle's impact on the dryer's surface (%) is calculated, its magnitude is found to be less when the initial feed moisture of 9 kg_w/kg_f is used. At higher initial feed moisture (> 9 kg_w/kg_f) content, air circulation is found to be minimum (0.0806) and maximum when feed moisture is 0.67 kg_w/kg_f. Thus, the initial feed moisture is found to be a significant parameter and it influences flow pattern in spray dryer. Since the air circulation rate is found to be higher at 0.67 kg_w/kg_f (optimum). This moisture content is considered for further investigation.

The knowledge of particle's impact position on the dryer's surface is important for design of the dryer chamber as it influences quality of the final product. Hence, wide range of particle sizes (50 μm - 600 μm) in the feed slurry (maltodextrin) are considered and their effect on the particle's impact position on the dryer's surface are calculated [optimized outlet nozzle location (a) & initial feed moisture, 0.67 kg_w/kg_f]. This is shown in Table 4.

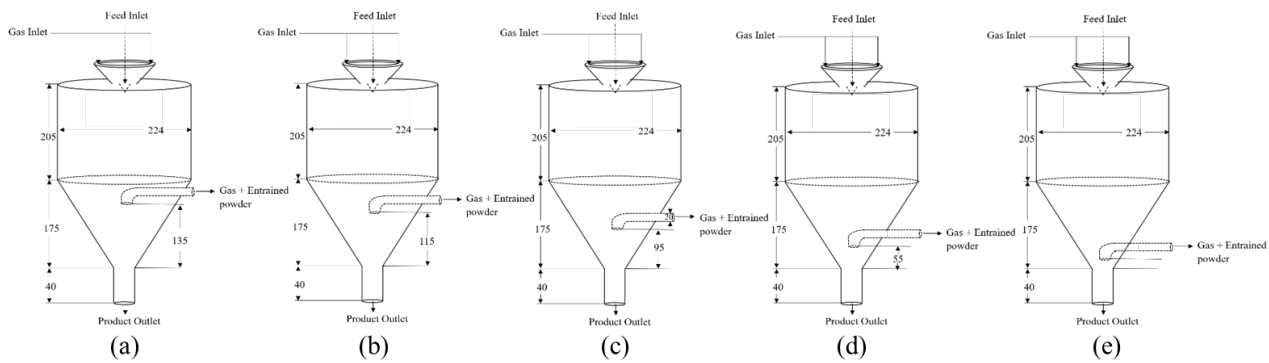

Fig. 5. Schematic of spray dryer with different air outlet locations (a-e).

Table 3. Effect of moisture content of the feed (initial) on evaporation rate, residence time of particle and impact positions on the dryer surface.

Moisture content (kg_w/kg_m)	Evaporation rate (10^5, kg s^{-1})	Air circulation rate (m^2 s^{-1})	Particle impact positions (%)		
			Cylindrical	Conical	Ceiling
0.11	2.77	0.1848	7.120	71.70	0.007
0.25	5.44	0.2727	6.000	63.38	0.006
0.67	10.66	0.3932	6.000	24.73	0.150
1.50	15.30	0.1636	2.370	21.62	0.150
4	19.82	0.2727	1.100	15.63	0.157
9	21.21	0.0806	0.005	07.87	0.0007

Table 4. Effect of particle size on air circulation rate, evaporation rate and particle impact positions on the dryer surface.

Particle size (μm)	Evaporation rate (10^5, kg s^{-1})	Air circulation rate (m^2 s^{-1})	Particle impact positions (%)		
			Cylindrical	Conical	Ceiling
50	10.66	0.3932	6.03	24.73	0.150
100	10.71	0.0319	16.0	21.48	0.001
200	10.83	0.0319	20.50	17.83	0
300	10.99	0.0874	21.10	17.35	0
400	10.99	0.0662	21.34	17.14	0
500	10.99	0.0159	21.78	17.76	0
600	11.00	0.0253	21.48	17.01	0

It is observed that the extent of particles that hits on the cylindrical section is lower for 50 μm as they dry at a faster rate. This is attributed to the smaller Stokes number. Hence, the air circulation rate is found to be higher for 50 μm size particles in comparison with other particle sizes. At 50 μm 24 % of particles hit the conical section due to weak air circulation rate and 6 % of particles hits the cylindrical section. A small portion i.e., less than 0.2 % of the particles, collides with the ceiling section of the spray dryer. It is also observed that no particle comes out of the product outlet chamber, but the particles colliding with the cylindrical and conical walls moves down to the product outlet.

Since a large number of particles strikes on the conical and cylindrical sections of the dryer, the conventional nozzle configuration used in the dryer is modified to improve evaporation rate (product quality). In the conventional nozzle, both feed mixture (maltodextrin slurry) and gas (hot air) are introduced into the flow domain through separate inlets. Accordingly, the interaction between particles and hot air takes place in the spray column. This nozzle is modified in such a way that the interaction between the particles and hot air takes places in the nozzle configuration itself. The proposed geometric configuration is shown in Fig. 6.

Here CFD simulations are performed for the optimized conditions. The predicted contours of velocity magnitude and hot air temperature are compared. This is shown in Fig. 7. The magnitude of air velocity in the core region is observed to be higher (20 m s^{-1}) for the spray dryer fitted with modified nozzle in compare with spray dryer with conventional nozzle. The temperature distribution is found to be uniform in the spray dryer with modified nozzle configuration.

Further, the performance of the proposed nozzle configuration is analysed by calculating particle impact (%), evaporation and air circulation rate. This is compared with spray dryer (conventional nozzle). This is depicted in Table 5. It is observed that the calculated particle impact percentage is lower and the evaporation rate is higher for the proposed nozzle configuration due to enhanced air circulation rate. Thus, the proposed

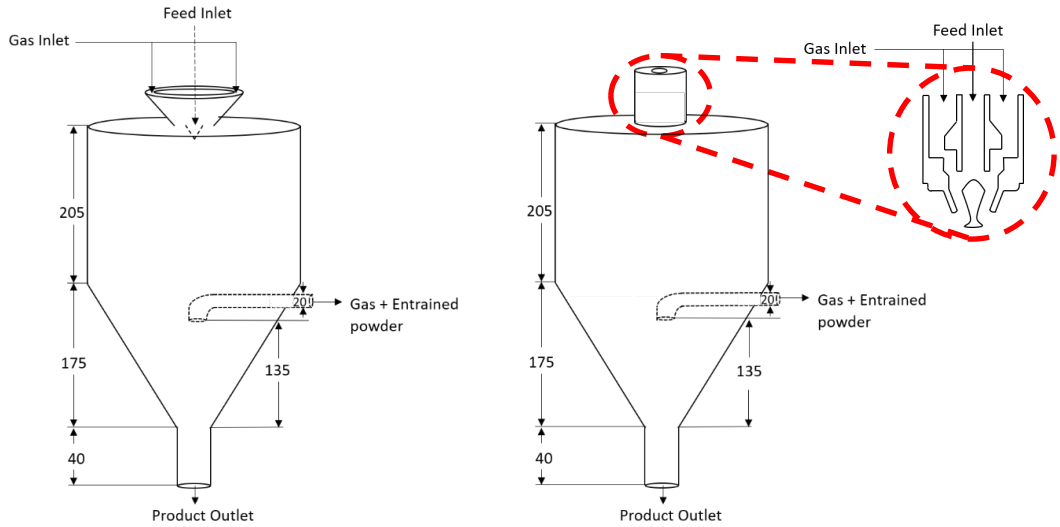

Fig. 6. Schematic of (a) conventional nozzle, (b) modified nozzle.

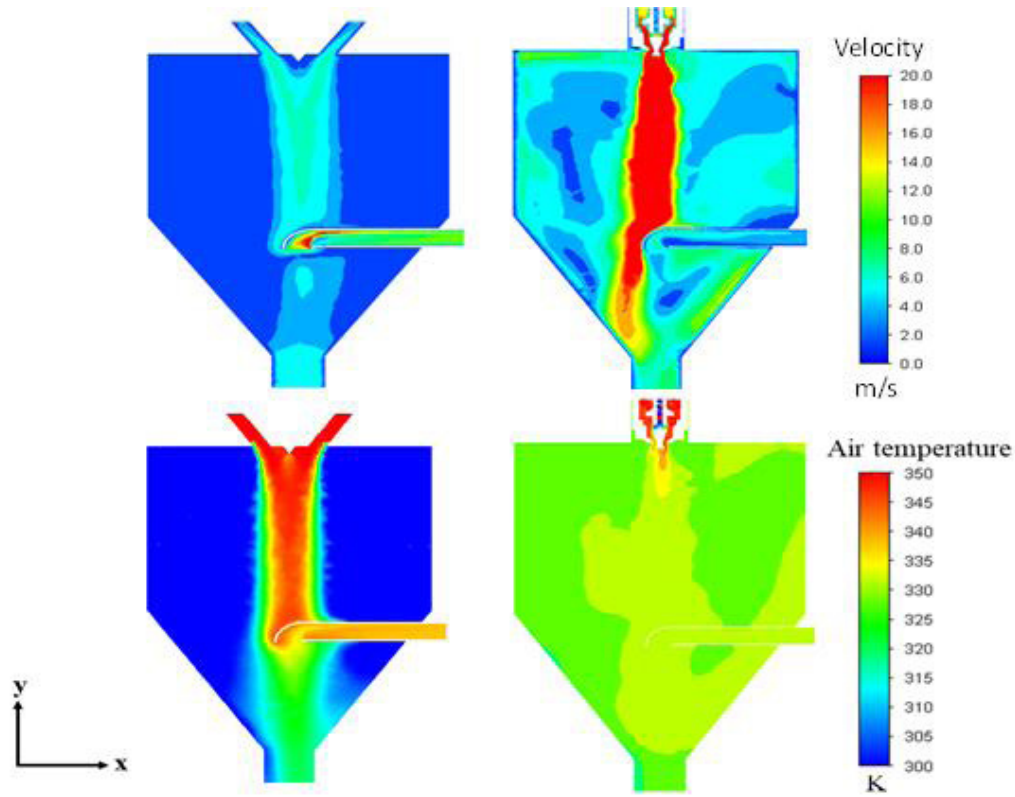

Fig. 7. Contour of velocity magnitude and temperature distribution (a) conventional nozzle, (b) modified nozzle.

Table 5. Effect of geometric configuration on particle impact positions, evaporation and air circulation rate.

Geometry	Particle impact positions (%)				Evaporation rate (10^5, kg s^{-1})	Air circulation rate (10^2, m^2 s^{-1})
	Cylindrical	Conical	Ceiling	Exit Nozzle		
Spray dryer (conventional nozzle)	6.03	24.73	0.15	4.70	9.73	0.3932
Spray dryer (proposed nozzle)	4.95	16.53	0.05	0	11.37	0.5942

nozzle configuration significantly influences the final product quality and supports drying of heat-sensitive food products.

CONCLUSIONS

The flow field in a spray dryer is investigated using a 3D CFD model using Euler-Lagrangian approach. The spatial variation of air velocity is analysed and found that its magnitude is high at the centre core of the dryer. The flow pattern is quantified by calculating air circulation. Accordingly, the optimum conditions for operation of spray dryer are identified. The effect of the outlet pipe location on the air recirculation rate and evaporation rate is analyzed. Accordingly, an optimum outlet pipe location is identified. Further, the effects of initial feed moisture content on evaporation rate and air circulation rate are analysed and found that its magnitude linearly increases with feed moisture. As the knowledge of the end position of particles is important for the design of spray dryer, extent of particle impact positions (%) on surface of the dryer is investigated. Its magnitude is found to be minimum at the cylindrical section of the spray dryer when particles of size 50 μm are used, due to smaller Stokes number. It is clear from the results that the extent of particles that hits on a spray dryer is strongly dependent on the particle size and the air flow pattern. Most of the particles (24 %) hit on the conical section of the dryer due to weak air circulation rate and increased particles residence time. This in turn influences the quality of the product, especially maltodextrin, when it is exposed to higher temperatures for longer time. To overcome this, the conventional nozzle configuration is modified in such a way that the interaction between feed mixture (slurry) and hot air occurs in the nozzle itself. The particle impact (%) on the dryer's surface is found to be lower when the proposed nozzle configuration is used. This study suggests that the modified nozzle configuration helps in obtaining higher collection efficiency of the product.

Acknowledgements

The authors express their gratitude to Mr. Sai Teja M. V. and Mr. Aarif for their support in drafting the manuscript.

REFERENCES

1. B.A. Ali, C.S. Kumar, S. Pushpavanam, Analysis of liquid circulation in a rectangular tank with a gas source at a corner, Chem. Eng. J., 144, 2008, 442-452, https://doi.org/10.1016/j.cej.2008.07.009.
2. J. J. Nijdam, B. Guo, D.F. Fletcher, T.A.G. Langrish, Lagrangian and Eulerian models for simulating turbulent dispersion and coalescence of droplets within a spray, Appl. Math. Model, 30, 2006, 1196-1211, https://doi.org/10.1016/j.apm.2006.02.001.
3. B.A.Ali, S. Pushpavanam, Analysis of unsteady gas–liquid flows in a rectangular tank: Comparison of Euler–Eulerian and Euler–Lagrangian simulations, Int. J. Multiph. Flow, 37, 2011, 268-277, https://doi.org/10.1016/j.ijmultiphaseflow.2010.10.002.
4. D.F. Fletcher, B. Guo, D.J.E. Harvie, T.A.G. Langrish, J.J. Nijdam, J. Williams, What is important in the simulation of spray dryer performance and how do current CFD models perform? Appl. Math. Model, 30, 2006, 1281-1292, https://doi.org/10.1016/j.apm.2006.03.006.
5. S. Cher Pin, W. Rashmi, M. Khalid, C.H. Chong, M.W. Woo, L.H. Tee, Simulation of spray drying on Piper betle Linn extracts using computational fluid dynamics., Int. Food Res. J., 21, 2014.
6. Masters, K, Spray Drying Handbook, Halsted Press, 1985.

7. S.N. Saleh, CFD simulations of a co-current spray dryer, Int. J. Chem. Mol. Eng., 4, 2010, 226-231.
8. S.N. Saleh, L.A. Hameed, CFD Simulation of Air Flow Patterns in a Spray Dryer Fitted With a Rotary Disk, Iraqi J. Chem. Pet. Eng., 17, 2016, 69-77.
9. V. Patil, A.K. Chauhan, R.P. Singh, Optimization of the spray-drying process for developing guava powder using response surface methodology, Powder Technol., 253, 2014, 230-236, https://doi.org/10.1016/j.powtec.2013.11.033.
10. M. Ali, T. Mahmud, P.J. Heggs, M. Ghadiri, A. Bayly, H. Ahmadian, L.M. de Juan, CFD simulation of a counter-current spray drying tower with stochastic treatment of particle-wall collision, Procedia Eng., 102, 2015, 1284-1294, https://doi.org/10.1016/j.proeng.2015.01.259.
11. D. Saha, S.K. Nanda, D.N. Yadav, Optimization of spray drying process parameters for production of groundnut milk powder, Powder Technol., 355, 2019, 417-424, https://doi.org/10.1016/j.powtec.2019.07.066.
12. B. Adhikari, T. Howes, D. Lecomte, B.R. Bhandari, A glass transition temperature approach for the prediction of the surface stickiness of a drying droplet during spray drying, Powder Technol., 149, 2005, 168-179, https://doi.org/10.1016/j.powtec.2004.11.007.
13. A. Gianfrancesco, C. Turchiuli, D. Flick, E. Dumoulin, CFD modeling and simulation of maltodextrin solutions spray drying to control stickiness, Food Bioprocess Technol., 3, 2010, 946-955, https://doi.org/10.1007/s11947-010-0352-2.
14. V. Francia, L. Martín, A.E. Bayly, M.J.H. Simmons, Agglomeration in counter-current spray drying towers. Part B: Interaction between multiple spraying levels, Powder Technol., 301, 2016, 1344-1358, https://doi.org/10.1016/j.powtec.2016.05.011.
15. L. Kavoshi, A. Rahimi, M.S. Hatamipour, CFD modeling and experimental study of carbon dioxide removal in a lab-scale spray dryer, Chem. Eng. Res. Des., 98, 2015,157-167, https://doi.org/10.1016/j.cherd.2015.04.023 .
16. ANSYS FLUENT 19 User's Guide (2019) Ansys Fluent Theory Guide. ANSYS Inc., USA
17. H. Versteeg, Introduction to Fluid Mechanics: by Y Nakayama and RF Boucher; Arnold, London, 1999, ISBN 0-340-67649-3., Flow Meas. Instrum., 11, 2000, 51-52, https://doi.org/10.1016/S0955-5986(99)00026-6.